Asian Journal of Chemistry; Vol. 25, No. 15 (2013), 8388-8392

ASIAN JOURNAL OF CHEMISTRY

http://dx.doi.org/10.14233/ajchem.2013.14761

Sensitive Electrochemical Determination of Luteolin in *Chrysanthemum morifolium* Ramat Using a Copper Nanocluster/Graphene-Modified Electrode

TIEJIN YANG* and DU JIANG

College of Chemistry and Chemical Engineering, Qiqihar University, Qiqihar-161006, P.R. China

*Corresponding author: E-mail: dujiang131@yahoo.com.cn

(*Received*: 1 November 2012; *Accepted*: 21 August 2013) AJC-13958

A simple and highly sensitive electrochemical method was developed for the determination of trace-level luteolin, based on the copper nanocluster/graphene-modified electrode. Scanning electron microscopy were used for the characterization of the distribution of the copper nanoclusters on the graphene matrix. The composite of the copper nanocluster/graphene was investigated by the electrochemical characterization of cyclic voltammetry and electrochemical impedance spectroscopy. The preliminary study shows that the sensor has synergistic electrocatalytic activity to the oxidation of luteolin. The linear range for the detection of the luteolin is 7.0×10^{-7}-3×10^{-6} M, a low detection limit of 3×10^{-8} M. Experiment results also showed that the sensor has good reproducibility and is interference free. The analytical performance of this sensor has been evaluated for detection of luteolin in *Chrysanthemum morifolium* Ramat as a real sample.

Key Words: Luteolin, Copper nanoclusters, *Chrysanthemum morifolium* Ramat, Graphene, Electrochemical analysis.

INTRODUCTION

The flower of *Chrysanthemum morifolium* Ramat (CM) has been used as Chinese traditional healthy food and medicine for hundreds of years. It is used for drink (just like tea) more usual than for medicine, especially in the summer. The flower of *Chrysanthemum morifolium* contains flavonoids, amino acids, vitamins and some trace elements. In addition to well-known antioxidant values[1,2], it has various biological features such as cardiovascular protection effects[3], protection against terminal tumors[4] and antiinflammatory features[5].

Flavonoids are a group of polyphenolic compounds widely distributed in plant. They are naturally occurring antioxidants to be utilized in a great number of health products[6]. Luteolin, a crucial member of the flavones, widely occurs in vegetables, fruits and natural herbal drugs, such as *Flos chrysanthemi, Caulis lonicerae japonicae* and *Flos lonicerae*. Aside from its effects of vasodilation[7] and cancer prevention[8], recent studies have also shown that it could enter the cellular nuclei and suppress the oxidative damage of DNA[9]. So far, a great deal of methods have been reported for the determination of luteolin in flavonoids, including high-performance liquid chromatography (HPLC)[10], capillary electrophoresis[11], spectrophotometry[12], gas chromatography (GC)[13], *etc*. Most of these methods have their own shortcomings, such as time-consuming, low sensitivity and complicate experimental process.

Recently, graphene has been considered as a ‘‘rising star” carbon material, attracting enormous interests. Graphene is made of monolayers of two-dimensional honeycomb graphite type carbon[14,15]. This unique nanostructure material has high surface area, excellent electrical conductivity and electron mobility at room temperature, robust mechanical properties and flexibility[16]. The special properties of graphene may provide insight to fabricate novel biosensors for virtual applications. The high surface area is helpful in increasing the surface loading of the target enzyme molecules on the surface. The excellent conductivity and small band gap are favourable for conducting electrons from the biomolecules. Recently, researches have demonstrated that graphene also possesses excellent electrochemical catalytic activity and should be a novel electrode modified material with excellent performance. For instance, Wang’s group found that graphene can improve sensitivity for lead and cadmium ion detections[17,18].

The nanomaterials such as graphene (GR) and transition metallic nanoparticles (NPs) have been widely applied in sensors and biosensors. Transition metallic nanoparticles, including gold, platimum, palladium, copper, nickel and silver, can be used to increase electrochemical activities with high sensitivity and fast amperometric method. In the current study, an effective sensor of luteolin was introduced with catalytic oxidation by electrodepositing the Cu nanoclusters onto the electrode modified with nafion-solubilized graphene. The sensor was then used for the analysis of the luteolin in real

Chrysanthemum morifolium Ramat and it provided high sensitivity and stability, fast current response and good reproducibility and selectivity.

EXPERIMENTAL

Luteolin (purity > 99 %) were obtained from J & K-ACIoS (serial number: 62696). Nf (5 %) was obtained from Aldrich (USA). $CuSO_4$ was purchased from Beijing Chemical Reagent (Beijing, China). All other reagents were of analytical grade and doubly distilled water was used throughout.

The electrochemical experiments were performed with a CHI660C electrochemical workstation (Shanghai, China). All experiments were carried out by a three-electrode system with a glassy carbon electrode (GCE, Φ = 3 mm) as the working electrode, a Pt wire as the auxiliary electrode and an Ag/AgCl/3 M KCl as the reference electrode.

Transmission electron microscopic (TEM) images were obtained by using a JEOL JEM-100SX microscope (Japan). The modified electrodes were characterized by SEM (S-4300, Hitachi High-Tech, Japan). The SEM equipped with EDS (EX-250, HORIBA, Japan) were employed for the composition analysis.

Sample preparation: *Chrysanthemum morifolium* were purchased from a QQHE pharmacy (Qiqihar, China). The luteolin sample was extracted from the *Chrysanthemum morifolium* as described. At first, the *Chrysanthemum morifolium* (2 g) was extracted with 50 mL of ethyl acetate at 80 ºC for 1.5 h. Then, the sample was cooled and filtered. The mixed suspension was centrifuged at 3000 rpm for 5 min. The supernatant was filtered through 0.45 μm membrane and diluted to 100 mL with water in a calibrated flask.

Synthesis of graphene: Graphite was put into a mixture of 12 mL concentrated H_2SO_4, 2.5 g $K_2S_2O_8$ and 2.5 g P_2O_5. The solution was heated to 80 ºC and kept stirring for 5 h using oil-bath. The mixture was diluted with deionized water (500 mL). The product was obtained by filtering using 0.2 μm nylon film and dried naturally. The product was re-oxidized by Hummers and Offeman method[19] to produce the graphite oxide. Exfoliation was carried out by sonicating 0.1 mg/mL graphite oxide dispersion for 1 h. Reduction of graphite oxide was carried out by adding 0.5 mL hydrazine into the solution of 50 mg graphite oxide powder in 20 mL water after sonicating for 1 h and kept stirring for 24 h at 50 ºC. Finally, black hydrophobic powder of graphene was obtained by filtration and dried in vacuum[20].

The morphology of the graphene was observed by TEM. Fig. 1 shows the TEM image of graphene nanosheets, illustrating the flake-like shapes of graphene.

Preparation of the modified electrodes: GC electrode was polished before each experiment with 1, 0.3 and 0.05 μm α-alumina powder (CHI Instrument, Shanghai, China) in sequence, rinsed thoroughly with doubly distilled water between each polishing step, ultrasonicated in 1:1 HNO_3, ethanol and doubly distilled water and allowed to dry at room temperature. Then 1 mg graphene was dispersed in 1.0 mL of 0.5 % nafion. The electrochemical synthesis of Cu nanoclusters on the graphene surface is shown in **Scheme-I**. GC electrode were modified by a 4 μL drop of graphene-nafion or nafion

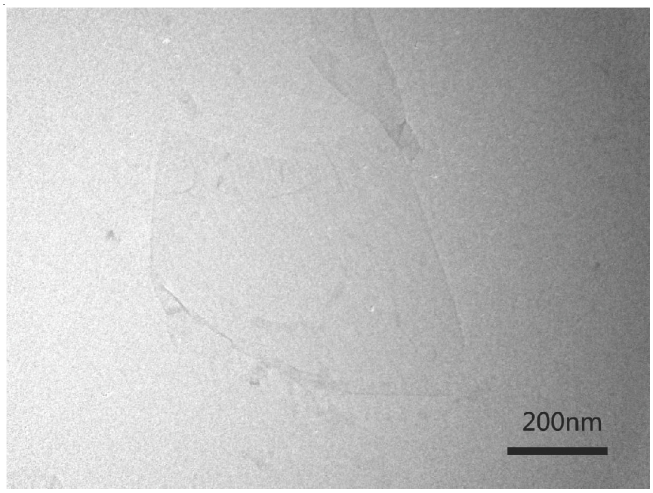

Fig. 1. TEM image of graphene in water

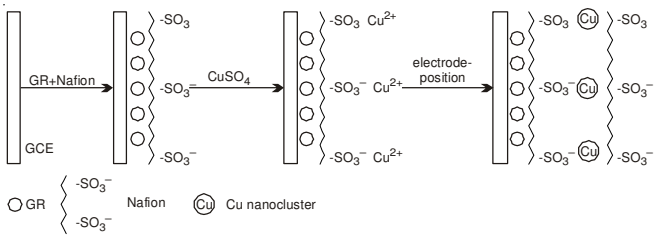

Scheme-I: Preparation process of the modified electrode

solution and dried in air. Thereafter Cu nanoclusters were deposited onto the above modified electrode from the solutions of 2.0 mM $CuSO_4$ in 0.1 M Na_2SO_4 under fixed applied potential of -0.2 V for 200 s, obtaining high sensitivity and reproducibility of the electrodes. The electrodes were rinsed with water, modified by a 4 μL drop of 0.5 % nafion on the surface and dried and stored at 4 ºC in a refrigerator.

RESULTS AND DISCUSSION

All the experiments were conducted at room temperature in a conventional electrochemical cell. The active surface area was estimated by steady-state voltammetry in a solution of 15 mM $K_4[Fe(CN)_6]$ with 0.2 M KCl as the supporting electrolyte. The electrochemical impedance spectroscopy (EIS) measurements were also performed in 10 mM $[Fe(CN)_6]^{3-/4-}$ solution containing 0.1 M KCl and plotted in the form of complex plane diagrams (Nyquist plots). They were recorded with a frequency range of 0.01 Hz to 10 kHz. The amplitude of the applied sine wave potential is 5 mV, with a formal potential 0.211 V. Cyclic voltammetry experiments were carried out in quiescent solution with a scan rate of 100 mV s^{-1} in an electrochemical cell filled with 5.0 ml of 50 mM PBS = 4. The current-time curves were recorded at 0.65 V under stirring. All experimental solutions were deoxygenated by high-purity nitrogen for 10 min.

Electrodeposition of Cu nanoclusters on graphene: Copper-nanoparticles were deposited onto graphene-GC electrode from the solutions of 2 mM $CuSO_4$ in 0.1 M Na_2SO_4 under fixed applied potential of -0.2 V for 200 s.

The prepared electrodes were characterized by TEM. Fig. 2 shows that Cu nanoclusters were deposited on the graphene matrix and that the size is 30-100 nm, indicating that the

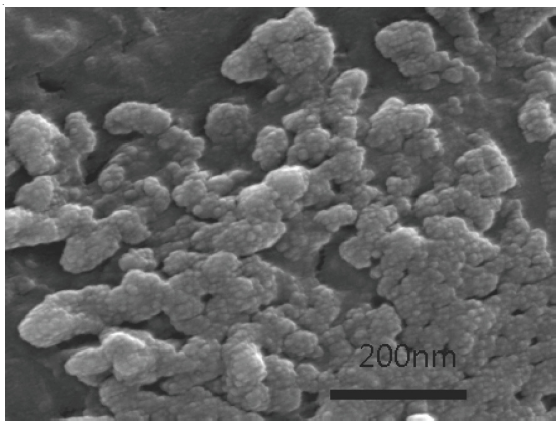

Fig. 2. SEM image of Cu nanoclusters on GR

larger size of copper nanoclusters may be an aggregation of a much finer size of copper nanoparticles. The results are ascribed to the following two possible reasons: on the one hand, as the size increases, some neighboring particles have a tendency to coalesce. On the other hand, considering the random distribution of particles, there certainly are some particles that suffer from marked diffusion interference and then form large-size Cu nanoclusters[21].

Fig. 3 illustrated the EDS of the copper nanoparticles/graphene modified electrode. The EDS conforms the additional signals corresponding to Cu elements besides the element .However from the percentages of Cu which are 90.01 %, it indicated that some Cu particles were oxidized. But the results further conform that the copper nanoparticles and graphene were modified on the glassy electrode.

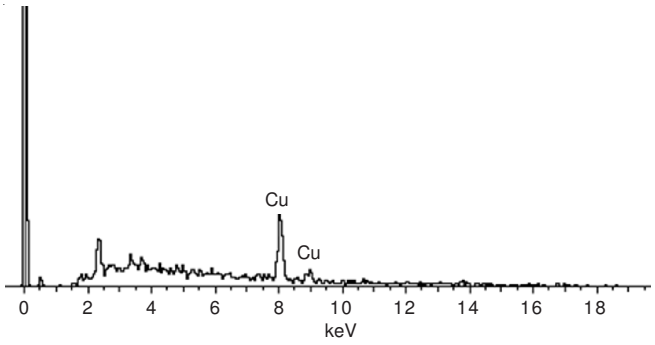

Fig. 3. EDS of Cu-NPs/GR/GCE

Electrochemical characterization: Fig. 4 compares the CV of a bare GCE with that of the four modified GCEr in 15 mM $K_4[Fe(CN)_6]$ with 0.2 M KCl at 20 mV s^{-1} Quasi-reversible one-electron redox behaviour of ferricyanide ion was observed on the bare GCE (Fig. 4 line a) with a peak separation (ΔEp) of 90 mV at 20 mV s^{-1}. After the electrode was modified with nafion, the lowest peak current (Ip) and the largest ΔEp were observed (Fig. 4 line b). Nafion is negatively charged and hinders the diffusion of ferricyanide ion toward the electrode surface. For the deposition of Cu nanoclusters on the nafion-modified electrode (Fig. 4 line c), the lowest current peak was increased and ΔEp was decreased compared with that of the nafion-modified electrode, indicating that Cu nanoclusters played a role in the increase of the electroactive surface area. Fig. 4 (line d) presents the voltammetric effect of ferricyanide

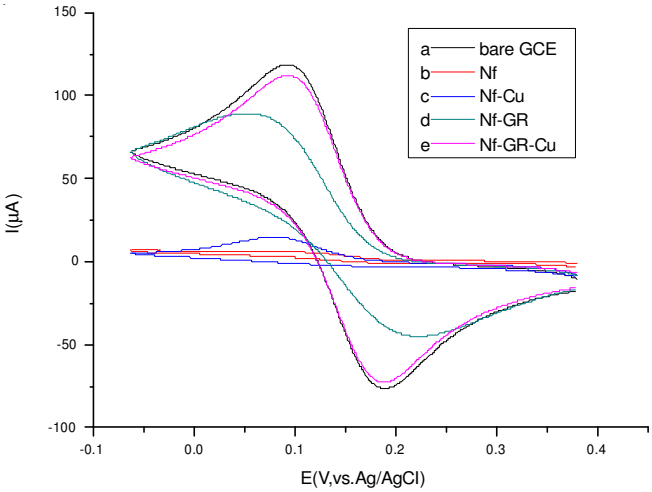

Fig. 4. CV of the electrodes in 15 mM $Fe(CN)_6^{4-}$ with 0.2 M KCl at 20 mV s^{-1} for bare GCE and four modified electrodes

ion on the graphene-nafion-modified electrode because graphene have a catalytically active surface and a very high aspect ratio. However, the lowest current peak of the modified graphene-nafion electrode was decreased compared with that of the bare GCE, due mainly to the blocking behaviour of nafion. With the application of copper-graphene-nafion composite film. The obtained voltammetric response was comparable to that of the bare electrode (Fig. 4 line e). The voltammograms show that copper-graphene-nafion film was effectively immobilized on the GCE surface and provided the necessary conduction pathways, resulting in promoting the electron transfer between the interface of analyte and electrode just like a nanoscale electrode. They also indicate that the electrode had a large electroactive surface area.

EIS was applied to monitor the whole process of the preparation of modified electrodes. This can give useful information of the impedance changes on the electrode surface between each step.

Fig. 5 shows the results of EIS for the bare GCE and four modified electrodes in the presence of equimolar $[Fe(CN)_6]^{3-/4-}$. The EIS includes a semicircular part and a linear part. The semicircular part at higher frequencies corresponds to the electron transfer limited process and the diameter is equivalent to the electron transfer resistance (Rct). The linear part at lower frequencies corresponds to the diffusion process. Using an appropriate equivalent circuit to fitting the data. During the fabrication, significant differences were observed. The electron transfer resistnace of the bare GCE is 226Ω (Fig. 5 line a).After GCE was modified with Nf, electron transfer resistnace increased markedly to 12,000 Ω, perhaps due to the Nf film acting as a barrier and blocking interfacial charge transfer (Fig. 5, line b).The results for the electrodes modified with graphene and Cu nanoclusters are shown in Fig. 5(lines c and d); electron transfer resistnace was decreased to 730 and 3400 Ω, respectively. When the copper-graphene-nafion composite was applied to modify the GCE, electron transfer resistnace was decreased to 400 Ω. The results show that the graphene or Cu nanocluster film was successfully immobilized on the GCE surface and the results are consistent with the CV results (Fig. 4).

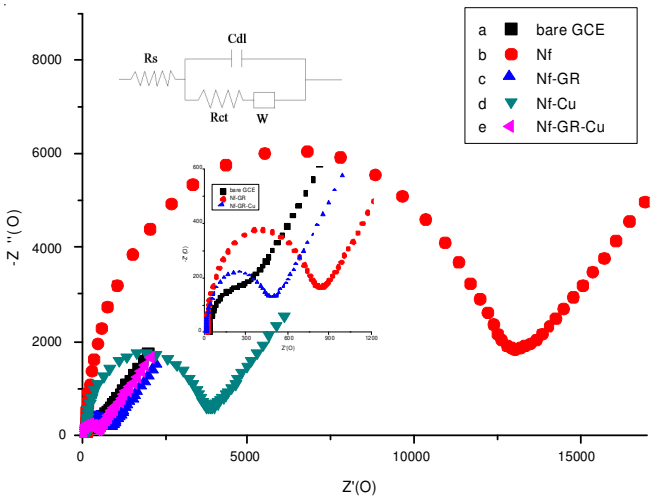

Fig. 5. Nyquist plots of EIS in 10 mM $Fe(CN)_6^{3-/4-}$ at 0.211 V for bare GCE and four modified electrodes. Inset: Magnified for bare GCE, Nf-GR-GCE and Nf-Cu-GR-GCE

Electrocatalysis of luteolin: Cyclic voltammetric studies were conducted in deoxygenated PBS = 4 with modified electrodes (Fig. 6). The current was reduced substantially after fabricating with nafion (Fig. 6, line a). When graphene-nafion film was formed on the GCE, the current was increased (Fig. 6, line b). The results revealed the electronic transfer between the graphene and the GCE surface. For the electrode modified with Cu nanoclusters, it displayed oxidation/reduction features of Cu and was similar to the CV of a bare Cu electrode (Fig. 6 line c).When fabricating Cu-GR-GCE, a large current was observed (Fig. 6, line d). Anodic peaks at -1 and 1 V are attributed to the conversion of Cu(0) to Cu(II). The cathodic peaks at 1 and -1 V are ascribed to the transition of Cu(II) to Cu(0).

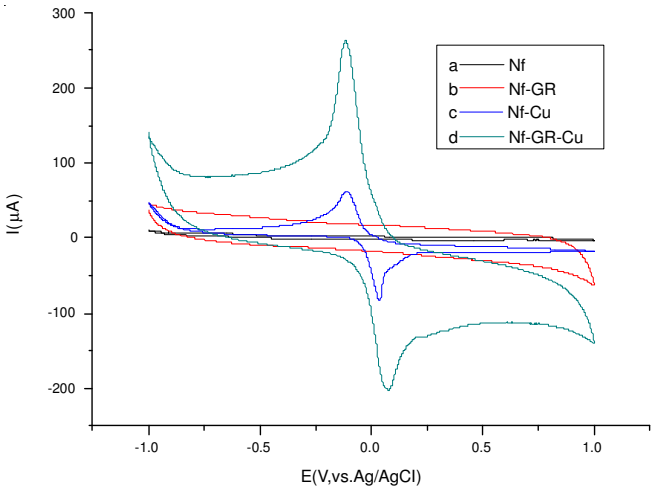

Fig. 6. CV of various modified electrodes in 50 mM PBS = 4 at 100 mV s^{-1}

Fig. 7 shows CV of the Cu-GR-GCE without and with 1.0 mM luteolin in 50 mM PBS = 4 at a scan rate of 100 mV s^{-1}. Although the exact mechanism for the oxidation of luteolin in PBS = 4 at Cu electrodes or Cu-modified electrodes is still not known with certainty, Cu(III) species have been proposed to act as an electron transfer mediator[22-24]. Fig. 7 inset illustrates the response current of luteolin by various modified electrodes at an applied potential of 0.8 V. No response current of nafion-modified GCE was observed and the response currents of

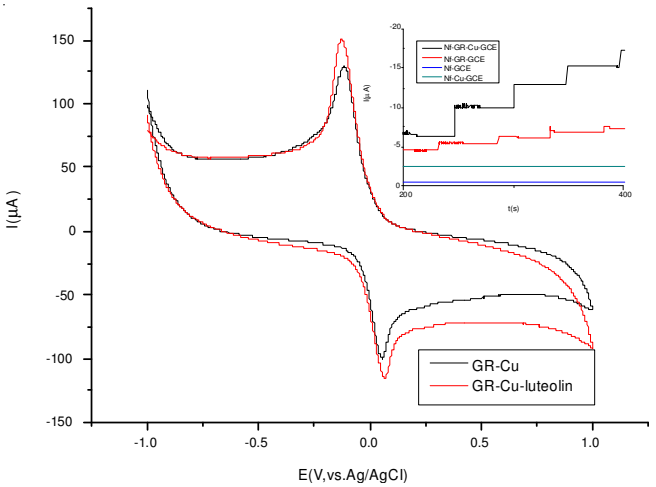

Fig. 7. CV of the Cu-GR-GCE without and with 1.0 mM luteolin in 50 mM PBS = 4 at 100 mV s^{-1} Inset: Steady-state current-time response of various modified electrodes to 1 mM luteolin in 50 mM PBS = 4 at 0.8 V

Cu-GCE and GR-GCE were small. Cu-GR-GCE had large and fast response currents.

Fig. 8 illustrates current-time plots for the sensor experimental conditions with successive step changes of luteolin concentration. The calibration curve for the sensor is shown in the left inset of the figure. The sensor displays a linear range (7.0×10^{-8}-3.0×10^{-6} M luteolin) with a correlation coeffcient of 0.9984, a detection limit of 3×10^{-8} M at a signal/noise ratio of 3. It can be attributed to the increase of electroactive surface area and the synergistic electrocatalytic activity by combining Cu nanoclusters with graphene. The relative standard deviation of eleven successive scans was 8.78 %, which indicated that the modified electrode had an excellent reproductively.

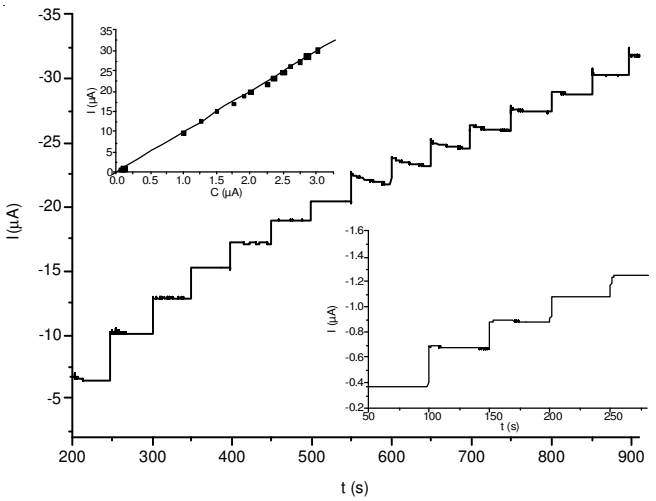

Fig. 8. Steady-state current-time responses of Nf-Cu-GR-GCE to various concentrations of luteolin in 50 mM PBS = 4 at 0.8 V. Left inset: Calibration curve. Right inset: Current-time response to 0.1 mM luteolin

Interferences: To evaluate the interferences of some foreign species on the determination of the current response of luteolin. Other possible interferents, such as 100 μM lysine, 100 μM citric acid, 100 μM glucose, 100 μM cyclodextrin, 100 μM lactose, 100 μM saturated starch, were individually

and simultaneously added into a standard solution containing 0.6 μM luteolin. The results indicated that on interference effect (signal change < 5 %) on the determination of luteolin was observed.

Determination of luteolin in *Chrysanthemum morifolium*: To demonstrate the performance of the proposed method in real sample analysis, the content of luteolin in *Chrysanthemum morifolium* was analyzed using current-time method based on the Nf-Cu-GR-GCE. It was found that the content of luteolin in *Chrysanthemum morifolium* was 3.12 ± 0.04 mg g^{-1} (n = 8), close to 3.52 ± 0.06 mg g^{-1} (n = 3) determined by high-performance liquid chromatography (HPLC). This means that the proposed voltammetry using Nf-Cu-GR-GCE is applicable for the fast determination of luteolin in *Chrysanthemum morifolium*. In addition, the recovery test was carried out by adding a known amount of luteolin standard into the sample and then analyzed according to the same procedure. The value of recovery is in the range from 95.5-101.4 %, also indicating that this method is reliable and feasible.

Conclusion

Copper nanoclusters have been electrochemically deposited on the layer of graphene matrix prepared on GCE, constructing a luteolin biosensor. The newly developed luteolin biosensor presents a number of attractive features such as high sensitivity and stability, good reproducibility and selectivity. It is ascribed to the increase of electroactive surface area, the synergistic electrocatalytic activity combining Cu nanoclusters with graphene and the three-dimensional porous structure of the Cu nanoclusters.The content of luteolin in *Chrysanthemum morifolium* was successfully determined with this Nf-Cu-GR-GCE, indicating that the Nf-Cu-GR-GCE would be promising for the fast voltammetric determination of the luteolin in *Chrysanthemum morifolium* and in other real samples.

REFERENCES

1. H.J. Kim and Y.S. Lee, *Planta Med.*, **71**, 871 (2005).
2. T. Wang, H.D. Jiang, Y.P. Ji and J.H. Xu, *J. Chin. Med. Mater*., **24**, 122 (2001) in Chinese.
3. H. Jiang, Q. Xia, W. Xu and M. Zheng, *Pharmazie*, **59**, 565 (2004).
4. M. Miyazawa and M. Hisama, *Biosci. Biotechnol. Biochem*., **67**, 2091 (2003).
5. M. Ukiya, T. Akihisa, K. Yasukawa, Y. Kasahara, Y. Kimura, K. Koike, T. Nikaido and M. Takido, *J. Agric. Food Chem*., **49**, 3187 (2001).
6. G.J. Volikakis and C.E. Efstathiou, *Talanta*, **51**, 775 (2000).
7. H.D. Jiang, Q. Xia, X.X. Wang and J.F. Song, *Pharmazie*, **60**, 444 (2005).
8. R.P. Samy, P. Gopalakrishnakone and S. Ignacimuthu, *Chem. Biol. Interact*., **164**, 1 (2006).
9. K. Kazuki, U. Mari, Y. Hiroaki and H. Takashi, *Arch. Biochem. Biophys*., **455**, 197 (2006).
10. S.M. Wittemer and M. Veit, *J. Chromatogr. B*, **793**, 367 (2003).
11. X.Q. Xu, L.S. Yu and G.N. Chen, *J. Pharm. Biomed. Anal*., **41**, 493 (2006).
12. I. Baranowska and D. Rarog, *Talanta*, **55**, 209 (2001).
13. C.S. Liu, Y.S. Song, K.J. Zhang, J.C. Ryu, M. Kim and T.H. Zhou, *J. Pharm. Biomed. Anal*., **13**, 1409 (1995).
14. A.K. Geim and K.S. Novoselov, *J. Nat. Mater.*, **3**, 183 (2007).
15. K.S. Novoselov, A.K. Geim, S.V. Morozov, D. Jiang, Y. Zhang, S.V. Dubonos, I.V. Grigorieva and A.A. Firsov, *Science*, **306**, 666 (2004).
16. S. Stankovich, D.A. Dikin, G.H.B. Dommett, K.M. Kohlhaas, E.J. Zimney, E.A. Stach, R.D. Piner, S.T. Nguyen and R.S. Ruoff, *Nature*, **442**, 282 (2006).
17. J. Li, S. Guo, Y. Zhai and E. Wang, *Anal. Chim. Acta*, **649**, 196 (2009).
18. J. Li, S. Guo, Y. Zhai and E. Wang, *Electrochem. Commun*., **11**, 1085 (2009).
19. W. Hummers and R. Offeman, *J. Am. Chem. Soc*., **80**, 1339 (1958).
20. Y. Wang, Y.M. Li, L.H. Tang, J. Lu and J.H. Li, *Electrochem. Commun.*, **11**, 889 (2009).
21. L. Cao, P. Diao, T. Zhu and Z. Liu, *J. Phys. Chem. B*, **108**, 3535 (2004).
22. V.G. Gavalas, S.A. Law, J.C. Ball, R. Andrews and L.G. Bachas, *Anal. Biochem*., **329**, 247 (2004).
23. Y. Lin, X. Cui and X. Ye, *Electrochem. Commun*., **7**, 267 (2005).
24. C.M. Welch and R.G. Compton, *Anal. Bioanal. Chem*., **384**, 601 (2006).